

Spring Technical Meeting
Eastern States Section of the Combustion Institute
March 8–11, 2020
Columbia, South Carolina

Impact of air splits in a dual-stream swirler on fuel-air mixing and thermoacoustic instability in a swirl stabilized high pressure combustor

Ashwini Karmarkar¹, Jisu Yoon², Isaac Boxx², and Jacqueline O'Connor^{1,}*

¹*Department of Mechanical Engineering, Pennsylvania State University, USA*

²*Institute for Combustion Technology, German Aerospace Centre (DLR), 70569 Stuttgart, Germany*

**Corresponding author: jxo22@psu.edu*

Abstract: Global instabilities in swirling flow fields can significantly impact fuel-air mixing in swirl stabilized flames, such as those found in gas turbine combustors. In this study, we investigate the interaction between shear layer instabilities and thermoacoustic oscillations and the impact of this interaction on the mixing of fuel and air in a realistic swirl stabilized combustor which employs two concentric swirling nozzles for air, separated by a ring of fuel injectors. The mean shear in the system is varied by systematically varying the air split between the two concentric nozzles. Transport and mixing of fuel is visualized by fluorescence of acetone, which is added with the fuel. Spectral characterization of acoustic measurements is done to identify the dominant modes in each of the cases and statistical analysis of the acetone signal is used to characterize fuel dispersion. Our results show that varying the air split between the two swirling nozzles, significantly affects the interaction dynamics between the thermoacoustic instability and hydrodynamic instability and the dispersion of fuel into the combustor. This characterization will help to identify the stability regimes for flames in complex combustor configurations.

Keywords: *Turbulent Flames, Fuel Air Mixing, Combustion Instability*

1. Introduction

Dual-annular swirlers are commonly used for flame stabilization in gas turbine combustors [1, 2]. In these injectors, air is split between two passages and swirled individually to increase the shear between the two streams and enhance fuel/air mixing and turbulence intensity in the flame region. The injector used in this study has a unique configuration where the air split between the two passages can be controlled independently [3], allowing us to better understand the impact of air split on combustion behavior. Here, the fuel is injected through 60 $0.5 \times 0.4 \text{ mm}^2$ channels in a ring on the dump plane between the two air circuits and so the interaction between the two air circuits directly impacts fuel/air mixing before the flame. This work follows previous investigations on this same injector by Geigle et al. [3].

In this configuration, variation in air split not only changes the amount of mean shear between the two air passages but also the swirl number, as the outer swirler has a swirl number of 0.79 and the inner swirler has a swirl number of 0.82. Varying these two parameters can have first-order impacts on both fuel-air mixing as well as flow field dynamics. Variation in the mean shear drives

the turbulence field development through the flow, and hence fuel-air mixing. Further, variations in the air split changes the overall swirl number of the flow, which can impact both shear layer dynamics as well as self-excited dynamics like the precessing vortex core. Previous work by our group [4] showed that variation in swirl number changed the receptivity of the shear layers in a swirling jet to external acoustic perturbations. Variation in the sensitivity of the shear layer to acoustics impacts the propensity for thermoacoustic instability in the system [5]. Thermoacoustic instability can also be affected by the level of fuel-air mixing ahead of the flame. Kypraiou et al. [6] showed variation in flame response to acoustic forcing with varying levels of premixing in a swirl-stabilized flame; they showed non-premixed flames respond more strongly to external perturbations than premixed flames.

Finally, variation in the level of swirl has significant impacts on global instabilities, particularly the precessing vortex core (PVC). Work by our group [7] and others [8] has shown that the intensity of the PVC increase with level of swirl, which in this injector would correlate with the air split between the two air circuits. Renaud et al. [9] and Anacleto et al. [10] both showed that a PVC could impact fuel/air mixing, resulting in variations in the thermoacoustic instability in the combustor.

The goal of this work is to understand the impact of air split on fuel/air mixing in this dual-annular swirler. Planar laser-induced fluorescence (PLIF) of acetone is used to image fuel/air mixing simultaneously with high-speed stereo particle image velocimetry (PIV). This initial study considers a the lower end of the injector fuel-split range to begin to correlate flow structure with fuel/air mixing and thermoacoustic instability.

2. Methods/Experimental

Experiments were conducted in a $68 \times 68 \times 120 \text{ mm}^3$ combustion chamber with optical access on all four sides and a cylindrical exhaust with a 40 mm diameter and a 24 mm length. Room-temperature air is fed separately to each passage in the dual-annular swirler, where the outer annulus has a 14.4 mm inner diameter and a 19.8 mm outer diameter, and the inner swirler has a 12.3 mm diameter. Gaseous C_2H_4 fuel is injected into slots between these two swirler passages. The combustion chamber is placed in a high-pressure vessel that raises the operating pressure to 5 bar. A more detailed discussion of the experimental facility is found in Geigle et al. [3].

Velocity data was obtained using high-speed stereo-PIV at 10 kHz using a dual-cavity Nd:YAG (Edgewave IS-6IIDE) laser with 2.6 mJ/pulse at 532 nm and a CMOS camera (LaVision HSS6). PIV data were processed using LaVision DaVis 8.1 with an interrogation window size of 16×16 and an in-plane spatial resolution of $1.2 \times 1.2 \text{ mm}^2$. Acetone PLIF data for the mixing study were obtained using a high-speed (10 kHz) dye laser (Sirah Credo) with $100 \mu\text{J}$ /pulse at 283.2 nm, which was pumped with a Nd:YAG laser (Edgewave IS-8IIE) with 4 mJ/pulse at 532 nm. Acetone-PLIF images were collected with a CMOS camera (LaVision HSS8 with HS-IRO) and a glass $f=85 \text{ mm}$, $f/1.2$ lens (Canon) that inherently filtered light below 350 nm, rejecting any laser-light reflections. The spatial resolution of the PLIF data is 0.0741 mm/pixel. A total of 10000 images were collected for both measurements.

3. Results and Discussion

Test Matrix

The data was taken at a pressure of 5 bar and the global equivalence ratio for all cases is 0.67. The air split is defined as the ratio of flow rate through the center nozzle to the total air flow rate. This air split is varied systematically and the measurements are used to make flow and mixing characterizations. The complete test matrix is shown in table 1.

Air Split	Diagnostic data
0.1	Acetone PLIF
0.2	Acetone PLIF, PIV
0.25	Acetone PLIF, PIV
0.3	Acetone PLIF, PIV
0.4	Acetone PLIF
0.5	Acetone PLIF

Table 1: Test matrix

Flow fields

The velocity vectors obtained from PIV were analyzed for three air split cases. Figure 1 shows the time-averaged streamwise velocity with varying air split. It can be seen that as the air split is increased, a recirculation zone develops along the centerline of the combustor. This is because the inner nozzle has a higher swirl number and increasing the flow through the center increases the net swirl in the system.

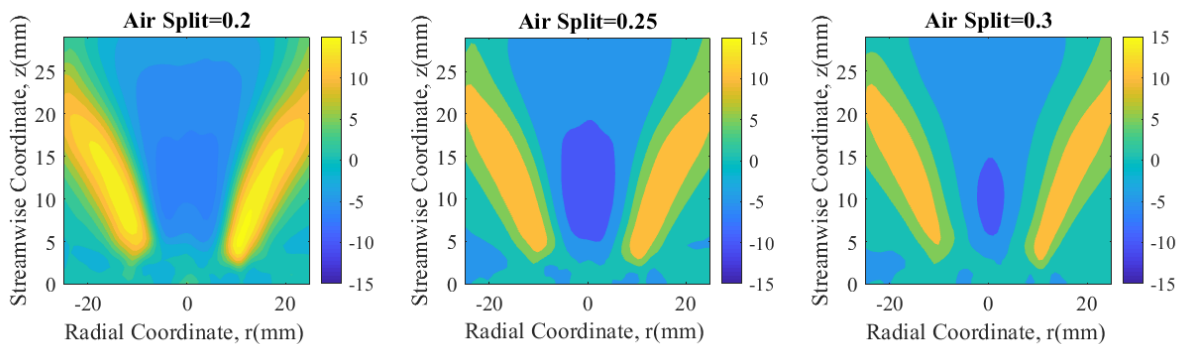


Figure 1: Time-averaged stream wise velocity(in m/s) for three air splits

Figure 2 shows the time-averaged vorticity for the three cases. The shear layer, created by the two air streams, can clearly be seen. As air split is increased, the shear layer weakens due to decreasing velocity gradient between the two concentric jets. It can also be seen that recirculation strength increases with increasing air split because the net swirl in the system is also increasing.

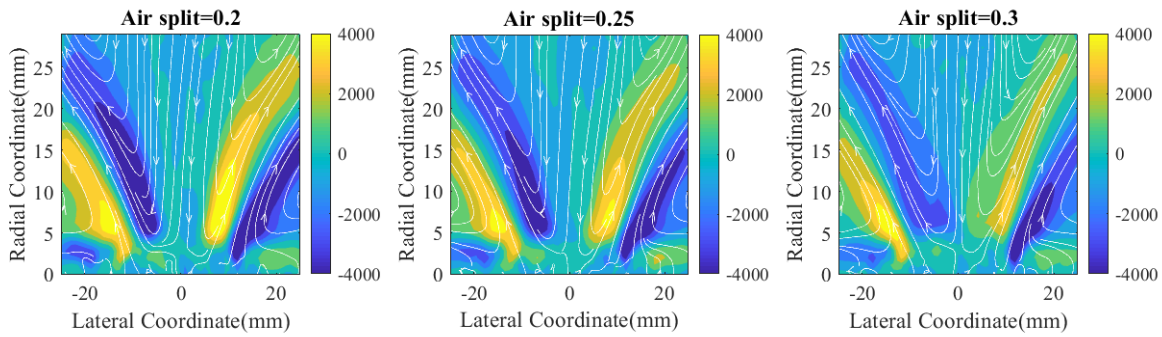


Figure 2: Time-averaged vorticity(in 1/s) for three air splits with streamlines

Fuel Air Mixing

The acetone PLIF images are analyzed to characterize the extent of fuel/air mixing. Figure 3 shows the time-averaged acetone PLIF images for five air split values; the PLIF signal scales with the concentration of the acetone in air. It can be seen that as air split increases, the fuel jets, initially located near $r/D = 0.5$, spread quickly in the radial direction. This mixing is the result of a number of different fluid-mechanic processes, including turbulence (particularly in the shear layers) and recirculation along both the centerline and in the corner recirculation zones.

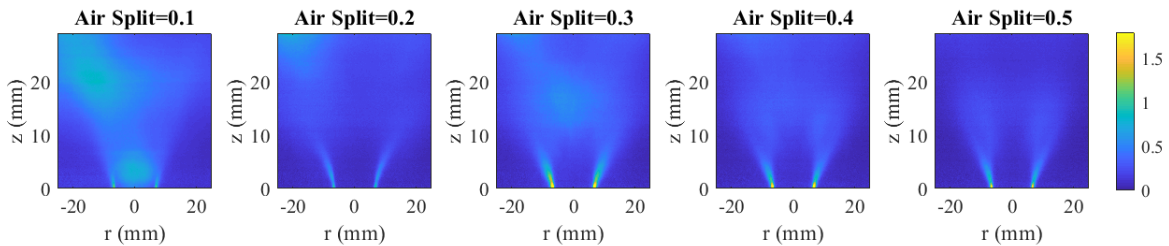


Figure 3: Time-averaged acetone PLIF images for five air splits

Figure 3 shows the time-averaged radial profile of the acetone signal intensity, normalized by its maximum value, for all air splits taken at three downstream locations. Close to the base, at $z/D=0.25$ it can be seen that the normalized signal intensities follow a similar trend for all cases except the case with air split of 0.1, which exhibits high acetone intensity along the centerline. This peak signal along the centerline is likely a result of the low air split, where very little flow enters the combustor through the inner swirler (10%) and the recirculation is relatively weak from the lower-swirl number jet from the outer nozzle. As such, fuel accumulates in this low-velocity zone. At further downstream distances, the fuel jets diverge and the peak concentrations move radially outward. In the 0.1 air split case, the maximum intensity is always in the centerline because of poor recirculation and low inner velocity. It can also be observed that the cases with higher air splits retain their peaks farther downstream because of strong recirculation and weaker shear layers.

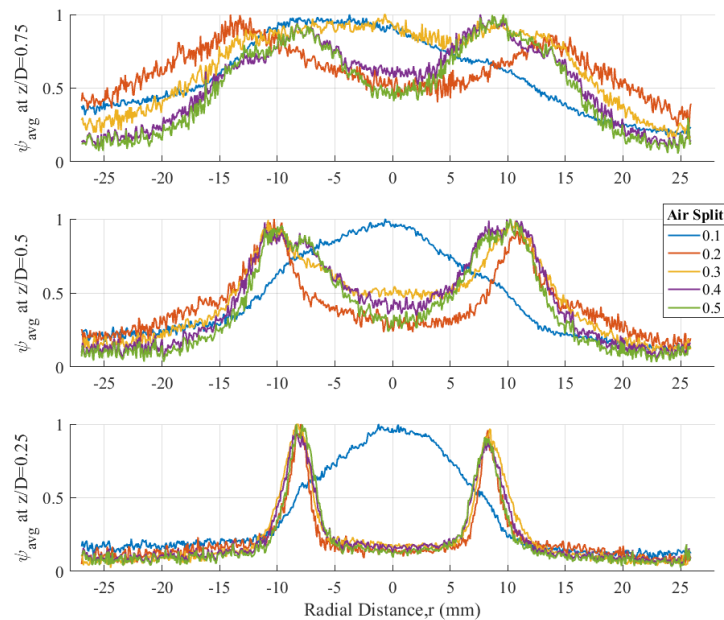


Figure 4: Time-averaged normalized signal intensity evaluated at different downstream distances for five air splits

In order to quantify dispersion, we perform a statistical analysis on the instantaneous acetone PLIF images. Figure 5 shows the probability density functions (PDF) of the normalized radially-averaged signal intensity of acetone for the five cases at different downstream locations. The distributions are calculated using 10000 PLIF images and are normalized by the maximum signal intensity. Close to the dump plane, at $z/D = 0.25$, it can be seen that for values of air split between 0.2 and 0.5, increasing air split causes the PDF peaks to move towards lower values of signal intensity. This indicates that mixing is enhanced by higher air splits, resulting in a more homogeneous mixture. It can also be seen that the peaks for lower air splits are broader. The exception to this trend is the case with an air split of 0.1. This anomalous behaviour could possibly be explained by the weak recirculation zone. When the acetone concentration distribution is integrated and normalized by the maximum (which is high because of fuel accumulation along the centerline), the normalized signal is consistently very low, which creates a sharp peak in the PDF.

Combustion Instability

Figure 6 shows the ensemble-averaged power spectral density calculated using the pressure measurements at different air splits. This ensemble averaged power spectral density is calculated by averaging the signal over 10 ensembles, each containing 200000 samples with a frequency resolution of 5 Hz. A peak at around 600 Hz can be seen in all cases, which is presumably the thermoacoustic mode. Another peak at around 1820 Hz is also consistently present. This peak corresponds to a global hydrodynamic instability. In the lower air split cases, the thermoacoustic mode is significantly stronger than the hydrodynamic instability, but this trend reverses as air split increases. In the higher air split cases, the dominant frequency is the hydrodynamic instability

Sub Topic: Turbulent Flames

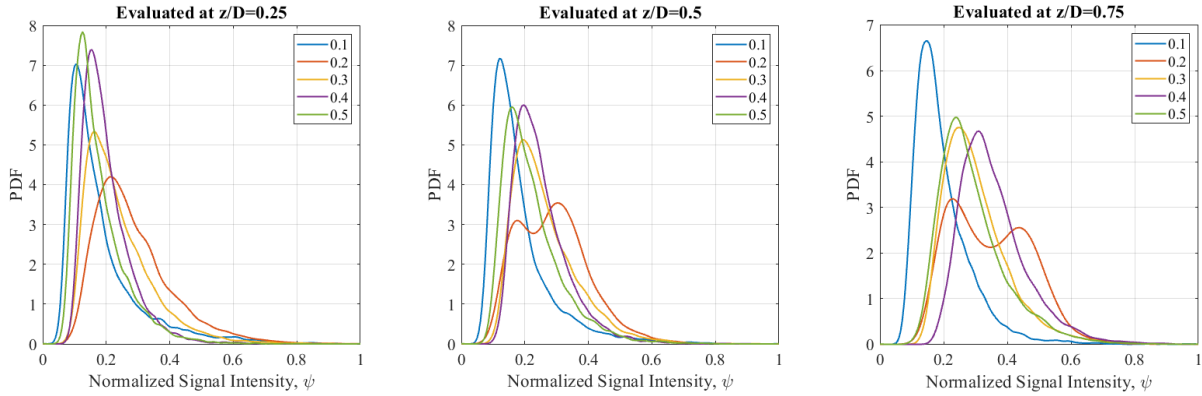


Figure 5: PDF plots of normalized signal intensity of radially-averaged acetone signal evaluated at various downstream locations

frequency, which is a consequence of increasing swirl as air split increases.

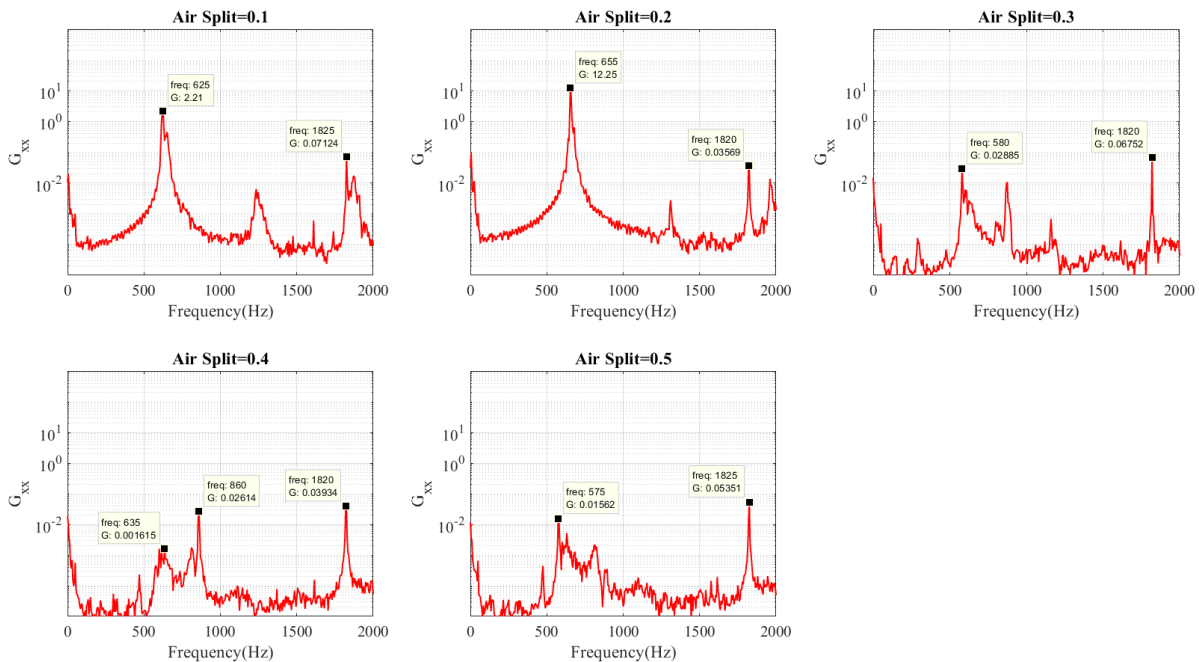


Figure 6: Power spectral density of combustor pressure traces for five select air splits

4. Conclusions

The goal of this study is to understand the impact that air split has on the dispersion of fuel into air in a dual-stream swirl combustor. By using flow field information, we have shown that the shear between streams weakens as the air split is increased, which causes the shear-generated turbulence to decrease. We characterize fuel dispersion using temporal distributions of normalized

signal intensity obtained from the acetone PLIF and show that increasing air split leads to enhanced dispersion. From the pressure spectra, it can be seen that in all the cases analyzed, both a thermoacoustic mode and a hydrodynamic instability mode are present. It is evident that the relative balance between the strength of the hydrodynamic instability mode and the thermoacoustic mode has a strong dependence on the air split. We can conclude that fuel/air mixing is impacted by the strength of the recirculation zone and the degree of mean shear in the system and there are different flow and flame regimes where one is dominant over the other. This insight can improve our current understanding of the combustion process in complex gas turbines and enable us to identify regimes with optimum fuel/air mixing, which will enhance flame stability and lead to more efficient combustion. Quantification of the degree of influence that each of these separate but connected dynamic processes can be used to design and model approaches for passive control of thermoacoustic instabilities.

5. Acknowledgements

This material is based upon work supported by the National Science Foundation under Grant CBET-1749679. Any opinions, findings, and conclusions or recommendations expressed in this material are those of the authors and do not necessarily reflect the views of the National Science Foundation.

References

- [1] G. Li and E. J. Gutmark, Geometry effects on the flow field and the spectral characteristics of a triple annular swirler, *ASME Turbo Expo* (2003).
- [2] H. Mongia, TAPS: a fourth generation propulsion combustor technology for low emissions, *AIAA International Air and Space Symposium and Exposition: The Next 100 Years* (2003).
- [3] K. P. Geigle, M. Köhler, W. O’Loughlin, and W. Meier, Investigation of soot formation in pressurized swirl flames by laser measurements of temperature, flame structures and soot concentrations, *Proceedings of the Combustion Institute* 35 (2015) 3373–3380.
- [4] B. Mathews, S. Hansford, and J. O’Connor, Impact of swirling flow structure on shear layer vorticity fluctuation mechanisms, *ASME Turbo Expo* (2016).
- [5] C. O. Paschereit, E. Gutmark, and W. Weisenstein, Excitation of thermoacoustic instabilities by interaction of acoustics and unstable swirling flow, *AIAA Journal* 38 (2000) 1025–1034.
- [6] A. Kypraiou A. M., A. P. M. Giusti, and E. Mastorakos, Response of flames with different degrees of premixedness to acoustic oscillations, *Combustion Science and Technology* 190 (2018) 1426–1441.
- [7] M. Frederick, J. Manoharan K. Dudash, B. Brubaker, S. Hemchandra, and J. O’Connor, Impact of precessing vortex core dynamics on shear layer response in a swirling jet, *Journal of Engineering for Gas Turbines and Power* 140 (2018) 061503.
- [8] K. Oberleithner, M. Sieber, C. Nayeri, C. Paschereit, C. Petz, H.-C. Hege, B. Noack, and I. Wygnanski, Three-dimensional coherent structures in a swirling jet undergoing vortex breakdown: stability analysis and empirical mode construction, *Journal of Fluid Mechanics* 679 (2011) 383–414.

Sub Topic: Turbulent Flames

- [9] A. Renaud, S. Ducruix, and L. Zimmer, Experimental Study of the Precessing Vortex Core Impact on the Liquid Fuel Spray in a Gas Turbine Model Combustor, *Journal of Engineering for Gas Turbines and Power* 141 (2019) 111022.
- [10] P. M. Anacleto, E. C. Fernandes, M. V. Heitor, and S. I. Shtork, Swirl flow structure and flame characteristics in a model lean premixed combustor, *Combustion Science and Technology* 175 (2003) 1369–1388.